Park *et al. Applied Biological Chemistry* (2022) 65:49
https://doi.org/10.1186/s13765-022-00711-z

KSABC
The Korean Society for Applied Biological Chemistry

ARTICLE Open Access

Crateva unilocularis Buch-Ham leaf extract improves glucose metabolism via regulation of insulin secretion and sensitivity in vitro and in vivo

Chul-Min Park[1,4†], Bong-Hwa Jeong[1†], Raj Bhesh Sharma[1], Hyun-Jung Kim[2], Dong-Wook Kim[1] and Dong-Young Rhyu[1,3*]

Abstract

Crateva unilocularis Buch-Ham has traditionally been used in Nepal for the treatment and prevention of diabetes. However, scientific verification through studies on the preventive effect of *C. unilocularis* on diabetes has not been done properly. In this study we investigated the effect of *C. unilocularis* leaf extract (CULE) on glucose uptake and insulin resistance. The effect of CULE on glucose uptake in an in vivo system was measured using zebrafish. In the cell-free system, enzymes activities related to diabetes were measured. Moreover, in the cell-cultured system, RIN-m5F pancreatic beta cells, 3T3-L1 adipocytes, and L6 myotubes were used to measure the effect of CULE on insulin secretion and glucose metabolism. CULE effectively enhanced glucose uptake in zebrafish larvae, and inhibited the activity of dipeptidyl peptidase-IV (DPP-IV) and protein tyrosine phosphatase-1B (PTP-1B) enzymes related to insulin secretion and insulin signaling activation. Also, CULE significantly increased insulin secretion with suppression of NO production in RIN-m5F pancreatic beta cells. In L6 myotubes and TNF-α-induced insulin resistance model of 3T3-L1 adipocytes, CULE significantly increased glucose uptake and immunofluorescence staining of glucose transporter (GLUT)4 protein. Furthermore, the regulatory response of glucose metabolism by CULE was a close correlation with the activation of insulin signaling (IRβ, PI3K, AKT) and 5′-AMP-activated protein kinase (AMPK)α and the reduction of p38 mitogen-activated protein kinase (MAPK) in TNF-α-induced insulin resistance model of 3T3-L1 adipocytes. Thus, our results suggest that CULE may act as a potential agent for the prevention and treatment of metabolic syndrome associated with type 2 diabetes.

Keywords: *Crateva unilocularis* Buch-Ham, Insulin secretion, Insulin sensitivity, Glucose metabolism, Zebrafish larvae

Introduction

Type 2 diabetes mellitus (T2D) is a metabolic disease that causes persistent hyperglycemia [1]. It is generally characterized by insulin secretion disorders and insulin resistance, although the exact cause is not clearly known up to now [1–4]. Currently, oral medications for glucose homeostasis of T2D can be divided into five classes: alpha-glucosidase inhibitors delaying the absorption of carbohydrates in small intestine; dipeptidyl peptidase-IV (DPP-IV) inhibitors, glucagon-like peptide-1 (GLP-1) receptor agonists, and sulfonylureas increasing the production of insulin in pancreas; biguanides reducing hepatic glucose production; thiazolidinediones improving insulin sensitivity in adipose tissue and skeletal muscle; and sodium-glucose linked transporter 2 (SGLT2)

†Chul-Min Park and Bong-Hwa Jeong are contributed equally to this work

*Correspondence: rhyudy@mokpo.ac.kr

[1] Department of Nutraceutical Resources and Institute of Korean Herbal Medicine Industry, College of Natural Sciences, Mokpo National University, 1666, Youngsan-ro, Muan-gun, Jeonnam 58554, Republic of Korea
Full list of author information is available at the end of the article

inhibitors reducing the absorption of glucose in kidney [5–7]. In clinical practices, antidiabetic drugs are used as a single medication or combination of medications to control blood glucose levels [8]. Therefore, the main strategy of this study is to find out how natural materials as novel oral agent of T2D affect the protein expression related to insulin secretion and insulin sensitivity (activation of insulin signaling or AMPK pathway) in tissues and organs involved in glucose metabolism.

Crateva unilocularis Buch-Ham belongs to the family *Capparaceae* (*Crateva*) and is known in China as "syu tau coi" [9]. *C. unilocularis* is also called a spider tree because its branch is like a spider's foot. As a folk medicine, the bark is used to stop abdominal pain and diarrhea, diuresis, fever, and stones, and the leaf decoction is used for urinary tract infections [10, 11]. In Nepal, the leaves are used to treat rheumatism, and the bark juice has been used for kidney disease, headaches, and diabetes [12]. It has been reported that the leaves and roots of *C. unilocularis* contain saponins, flavonoids, phytosterols, oils, and phenolic compounds, and *C. unilocularis* extracts exhibits excellent DPPH radical scavenging activity and anti-obesity effects [9, 10, 13]. However, research papers of *C. unilocularis* on diabetes have not yet been published. Therefore, there is a need to establish the scientific evidences for the biological effect of reducing blood glucose levels. We investigated the effects of *C. unilocularis* leaf extract (CULE) on glucose homeostasis though regulation of insulin release and insulin sensitivity in RIN-m5F pancreatic beta cells, L6 myotubes, 3T3-L1 adipocytes, and zebrafish (*Danio rerio*).

Material and methods

Chemicals

Dulbecco's modified Eagle's medium (DMEM), newborn calf serum (NBCS), fetal bovine serum (FBS), phosphate-buffered saline (PBS), trypsin, and penicillin–streptomycin were obtained from Hyclone (Logan, UT, USA). Dexamethasone (DEX), insulin, 3-isobutyl-1-methyxanthine (IBMX), β-actin antibody, 3-(4,5-dimethylthiazol-2-yl) 2,5-diphenyltetrazolium bromide (MTT), N omega-Nitro-L-arginine methyl ester hydrochloride (L-NAME), and rosiglitazone were purchased from Sigma-Aldrich (St. Louis, MO, USA). 2-(N-(7-nitrobenz-2-oxa-1,3-diazol-4-yl)-amino)-2-deoxyglucose (2-NBDG) was purchased from Invitrogen (Carlsbad, CA, USA). Tris (hydroxymethyl) aminomethane (Tris) base, glycine, and sodium dodecyl sulfate (SDS) were purchased from the Promega Corporation (Madison, WI, USA), and nitrocellulose membranes were purchased from Bio-Rad (Hercules, CA, USA). The western blot detection kit and lysis buffer were purchased from iNtRON Biotechnology (Burlington, MA, USA). Insulin receptor β (IRβ;#3025), phospho-phosphoinositide 3-kinases (p-PI3K;#4228), PI3K (#4292), phospho-AKT (p-AKT;#9271), AKT(#9272), glucose transporter (GLUT4;#2213), phospho-p38 mitogen-activated protein kinase (p-p38 MAPK;#4511), p38 MAPK (#8690), phospho-AMP-activated protein kinase α (p-AMPKα;#2535), and AMP-activated protein kinase α (AMPKα;#2532) antibodies were purchased from Cell Signaling Technology (Danvers, MA, USA). GLUT4, insulin receptor substrate-1 (IRS-1), and β-actin primers were purchased from Integrated DNA Technologies (IDT, Korea).

Extraction of C. unilocularis leaves

The leaves of the *C. unilocularis* Buch-Ham plant were harvested and dried in Baglung, Nepal in July 2014. Dried *C. unilocularis* leaves (400 g) and 2L of distilled water (DW) were added together, followed by hot water extraction at 100 °C. This process was repeated twice for 60 min to obtain an extract. The extract was filtered with a filter paper and concentrated on a rotary evaporator (EYELA, Tokyo, Japan) in a water bath below 45 °C. The concentrate was lyophilized and powdered and diluted to various concentrations for use in the experiments. The *C. unilocularis* leaf extract was named CULE. The yield of the extract was determined to be 12% (48 g). *C. unicolularis* was reviewed and certified by Dr. Kim Hui, Mokpo National University, Korea. The voucher specimens of the *C. unicolularis* plant were kept in the laboratory for further documentation [14].

High-performance liquid chromatography (HPLC) analysis

HPLC analysis was carried out in the Alliance HPLC system (Waters, MA, USA) with a PDA detector (190–500 nm) using a Capcell Pak C18 (250 × 4.6 mm, 5 µm, Shiseido, Japan). Samples and standard solutions were eluted by an isocratic solvent system (H_2O: 5% acetic acid: acetonitrile = 40: 30: 30) with the flow rate of 0.8 mL/min at 35 °C. The standard solutions of quercetin and CULE were prepared as follows; 10 mg of quercetin was dissolved in methanol and prepared as a stock solution with the concentration of 1,000 ppm using a 10 mL volumetric flask. Then, it was diluted to prepare a standard solution (20 to 500 ppm). For the CULE sample, 1 g of CULE was extracted with 40 mL of 60% EtOH and 5 mL of 6 N HCl under reflux condition for 2 h at 95 °C, and made into 50 mL of final volume with 60% EtOH. The standard solutions and test solutions were filtered with 0.45 µm nylon filter and injected with a volume of 10 µL. All HPLC chromatograms were extracted under 370 nm. The calibration curve for quercetin was recorded using concentrations (X) and peak areas (Y).

Measurement of survival rate and 2-NBDG uptake analysis in zebrafish

Wild-type adult zebrafish received from the Seoul Institute of Science and Technology for Environmental Toxicity and Health Research Labs were maintained in 14 h light/10 h dark cycles, at a temperature of 28 °C and a pH of 7.0, circulating in a tank with a filtration system (Zebtec Stand Alone, Italy). Embryo collection was performed by placing adult male and female zebrafish into the embryo collection tank 24 h before the experiment and collecting the embryos within 2 h of the photoperiod of the next day. After 6 h post-fertilization (hpf), 100 µL of E2 medium (zebrafish embryo medium) was added to each well of each 96-well plates and one embryo was transferred in each well. On 7-days post-fertilization (dpf), zebrafish larvae were exposed to CULE for 24 h, and the survival and deformity rates were observed compared to the control group [15].

Embryos obtained through mating of male and female zebrafish were grown up for 7 days. Then, on day 7 dpf, zebrafish larvae were exposed to CULE for 24 h. After 24 h, zebrafish larvae were treated with 600 µM 2-NBDG for 3 h and washed 3 times with E2 medium. The zebrafish larvae after washing were observed and photographed under a fluorescence microscope (Leica, Wetzlar, Germany). The fluorescence intensity of the zebrafish larvae was quantified using the ImageJ program [15]. All experiments were performed in accordance with the guidelines of American Veterinary Medical Association and Mokpo National University for laboratory animal.

Measurement of protein tyrosine phosphatase 1B (PTP-1B) and dipeptidyl peptidase IV (DPP-IV) enzyme activities

The activation of DPP-IV were made in 25 µL of 50 mM HEPES buffer (pH 7.4) containing Gly-Pro-AMC (1 mM) and 10 µL of rat serum to which CULE was added and reacted for 1 h. The reaction was terminated by adding 70 µL of 3 M acetic acid, and fluorescence was measured at an excitation (ex) wavelength of 370 nm and an emission (em) wavelength of 440 nm using a multilabel plate reader (VICTOR 3 V, PerkinElmer Inc., Waltham, MA, USA). The activation of PTP-1B was initiated by adding 10 µL of CULE, 3 µL of reaction buffer (50 mM citrate, pH 6.0) containing 0.1 M NaCl, 1 mM EDTA, and 1 mM dithiothreitol (DTT), 35 µL of DW, 2 µL of PTP-1B enzyme, and 50 µL of 20 mM p-nitrophenyl phosphate (p-NPP) and incubated at 37 °C for 30 min. After terminating the reaction by adding 100 µL of 1 M NaOH, the absorbance was measured at 405 nm using Immuno-mini NJ-2300 microplate reader (Nalge Nunc, Tokyo, Japan) [16].

Cell culture and differentiation

RIN-m5F pancreatic beta cells, L6 myoblasts, and 3T3-L1 preadipocytes were obtained from the American Type Culture Collection (ATCC, Manassas, VA, USA). RIN-m5F pancreatic beta cells and L6 myoblasts were cultured in DMEM containing 10% FBS, 100 µg/mL streptomycin, and 100 units/mL penicillin and incubated in 95% oxygen and 5% CO_2 at 37 ℃. 3T3-L1 preadipocytes were cultured in DMEM containing 10% NBCS. All cell lines were supplemented with fresh medium every 2 days, and used in the experiments.

The procedure for the differentiation of 3T3-L1 preadipocytes and L6 myoblast is as follows. 3T3-L1 preadipocytes were seeded in a 6-well plates at 1×10^5 cells/well and cultured in differentiation medium (5 µg/mL insulin, 1 µM DEX, and 0.5 mM IBMX in DMEM with 10% FBS) for 2 days when the cell growth reached 90–100% confluency. After 2 days of differentiation, the medium was exchanged with DMEM with 10% FBS containing 5 µg/mL insulin, and used for the experiment four days later. Fresh DMEM with 10% FBS was added every 2 days. L6 myoblasts were seeded into 6-well plates at 1.8×10^4 cells/well, when the cells reached about 80–90% confluency, the medium was changed to DMEM with 2% horse serum (HS) and the cells were allowed to differentiate for 7 days.

Insulin resistance cell model

Recombinant murine tumor necrosis factor-α (TNF-α, 315-01A; PeproTech, NJ, USA) at a concentration of 10 ng/mL was added to 3T3-L1 adipocytes, which were completely differentiated into adipocytes, and then used as a cell model in which insulin resistance was induced after 48 h with an exchange of fresh medium every 24 h [17].

Cell viability

RIN-m5F pancreatic beta cells were seeded in 96-well plates at 1×10^5 cells/well, incubated for 12 h, reacted for 3 h with various concentrations of CULE, then reacted with IL-1β (2 ng/mL) and IFN-γ (100 U/mL) for 48 h. 3T3-L1 adipocytes and L6 myotubes were aliquoted at 5×10^3 or 1×10^3 cells/well in 96-well plates and incubated for 24 h before adding various concentrations of CULE. After the reactions, MTT (1 mg/mL) solution was added for 3 h and the absorbance was measured at 540 nm (Immuno-mini NJ-2300 microplate reader, Nalge Nunc, Tokyo, Japan).

Measurement of NO and insulin

RIN-m5F pancreatic beta cells were seeded in 96-well plates at 1×10^5 cells/well and incubated for 12 h. Then,

IL-1β (2 ng/mL) and IFN-γ (100 U/mL) were added along with various concentrations of CULE. After reacting for 48 h, the same amount of cell culture medium and Griess solution was added per well and the absorbance was measured at 540 nm after 5 min using the Immuno-mini NJ-2300 microplate reader (Nalge Nunc, Tokyo, Japan). NO production was calculated using a standard curve generated using $NaNO_2$ standard solution.

Insulin secretion analysis was conducted under the same conditions and the insulin content secreted into the cell culture was measured using a Rat Insulin ELISA Kit (Mercodia, Uppsala, Sweden). L-NAME (1 mM) was used as a positive control.

2-NBDG uptake analysis

After differentiation into 3T3-L1 adipocytes and L6 myotubes in a black 96-well plates, the cells were treated with different concentrations of CULE and incubated for 24 h. Then, the cells were treated for 30 min with 80 μM (L6 myotubes) or 150 μg/mL (3T3-L1 adipocytes) 2-NBDG. After washing three times with PBS, fluorescence was measured at an excitation (ex) wavelength of 485 nm and an emission (em) wavelength of 535 nm using a Perkin-Elmer VICTOR 3 V, (PerkinElmer Inc.; Waltham, MA, USA). The fluorescence intensity reflected the glucose uptake of 2-NBDG into the 3T3-L1 adipocytes and L6 myotubes. Insulin (IN, 100 ng/mL) and rosiglitazone (RSG, 5 μM) were used as positive controls [18].

Immunofluorescence staining

After differentiating 3T3-L1 preadipocytes and L6 myoblasts on a glass cover slide, cells were treated with various concentrations of CULE and incubated for 24 h. After the experiment was completed, the coverslip was transferred to a 6-well plates, washed with PBS, and a 4% paraformaldehyde solution was added to fix the cells. The fixed cells were washed with 0.2% Triton X-100 and washed again with PBS. The primary and secondary antibodies were added to the washed coverslip, incubated, and washed with PBS. Then, a small amount of mounting medium was sprayed on a glass cover slide, and the fluorescently stained cells were photographed using LMS-700 (Carl Zeiss, Gottingen, Germany).

Reverse transcription-PCR analysis

TRIzol reagent (1 mL) was added to L6 myotubes after the experimental treatments and the cells were homogenized. Then, 0.2 mL of chloroform was added and gently mixed, followed by centrifugation at 12,000 g × 4 ℃ for 15 min. Isopropanol (0.5 mL) was added to the supernatant and the mixture was vortexed and stored at 25 ℃ for 5–10 min before centrifuging at 12,000 g × 4 ℃ for 8 min. The supernatant was removed, 1 mL of 75% ethanol was added, vortexed, and washed twice at 12,000 g × 4 ℃ for 5 min. After washing, the ethanol was removed, the sample was air-dried for 3–5 min, and 30–50 μL of diethyl pyrocarbonate (DEPC) was added and stored at -20 °C until used for the experiments. RNA was quantified by measuring the absorbance at wavelengths of 260 and 280 nm using a Nanodrop spectrometer (St. Louis, MO, USA, Sigma-Aldrich). The Diastar™2X OneStep RT-PCR Premix Kit (Biofact, Daejeon, Korea) was used to synthesize cDNA from total RNA (25 ng) by adding 3 μL of RNA and 1 μL of primer to a total 30 μL reverse transcription reaction. The base sequence of each primer was as follows: The forward sequence of GLUT4 was 5'-CCT GCC CGA AAG AGT CTA AAG C-3', and the reverse sequence was 5'-ACT AAG AGC ACC GAG ACC AAC G-3'; The forward sequence of IRS-1 was 5'-AGA GTG GTG GAG TTG AGT TG-3', and the reverse sequence was 5'-GGT GTA ACA GAA GCA GAA GC-3'; The forward sequence of β-actin was 5'-TGC CCA TCT ATG AGG GTT ACG-3' and the reverse sequence was 5'-TAG AAG CAT TTG CGG TGC ACG-3'. PCR analysis was carried out for 45 min by reacting for 30 min at 50 ℃, 15 min at 95 ℃ and denaturing for 1 min at 95 ℃, then attaching for 1 min at 55 ℃ and extending for 2 min at 72 ℃. The PCR products were electrophoresed on 1.5% agarose gel stained with RedSafe™ nucleic acid staining solution (iNtRON, Seongnam, Gyeonggi, Korea), and β-actin was used as a control for the amplified genes.

Western blot analysis

3T3-L1 adipocytes were washed twice with PBS. Lysis buffer was then added and dissolved at 4 °C for 10 min and the mixture was centrifuged at 13,000 rpm × 4 °C for 20 min to recover supernatant protein and the amount was quantified. The lysate (30 μg/mL) was mixed with SDS loading buffer (1 M Tris, 50% glycerol, 10% SDS, and 1% bromophenol blue), heated at 95 ℃ for 10 min, and electrophoresed on 10% SDS polyacrylamide gels. The gels were transferred to polyvinylidene difluoride (PVDF) membranes (Merck Millipore, Burlington, MA, USA). Five percent BSA was added to TBS-T (1 M Tris, 5 M NaCl, and 0.05% Tween 20) buffer and used to block the membranes for 1 h. After washing three times with TBS-T buffer, primary antibody (IRβ 1: 1000, p-PI3K 1: 500, PI3K 1: 1000, p-AKT 1: 1000, AKT 1: 1000, GLUT4 1: 500, p-AMPKα 1: 500, AMPKα 1: 500, p-p38 1: 500, p38 1: 1000, β-actin 1: 5000) was added and incubated overnight,

and the membranes were washed three times with TBS-T buffer. Then, they were reacted with a secondary antibody (goat anti-mouse 1: 1000 or anti-rabbit 1: 1000) containing peroxidase for 2 h and visualized using a western blot detection kit. The reactions were analyzed using UVP image analysis software (VisionworkTMLS, Fisher Scientific, UK) [19].

Statistical analyses

All experimental results are expressed as the mean ± standard error (SE). The difference between the groups was analyzed by one-way analysis of variance (ANOVA) using GraphPad Prism and the Dunnett post-test test. Comparison of the means of two independent sample variables were analyzed using an unpaired t-test.

Results

Effects of CULE in zebrafish larvae

We measured the effect of CULE on glucose uptake in zebrafish larvae to secure the scientific basis for traditional knowledge of folk remedies before cell experiments. We observed the effects of CULE on survival, malformation, and glucose uptake in zebrafish larvae. As a result, no changes of survival and malformation rate were observed at different concentrations (25, 100, 400, and 800 μg/mL) of CULE compared to control group (Fig. 1A, B). Glucose uptake ability in cells or zebrafish larvae plays a fundamental role in screening antidiabetic candidates. 2-NBDG as a glucose fluorescent probe has widely been used to monitor glucose uptake. CULE-treated zebrafish larvae produced significant glucose uptake with a dose-dependent manner compared to control (Fig. 1C, D). Thus, CULE was identified as effective materials for inducing glucose uptake.

Effect of CULE on DPP-IV and PTP1B enzyme activities

The PTP-1B and DPP-IV enzyme activities have well-known as a potential drug target for the treatment of type 2 diabetes. PTP1B plays an important role in insulin resistance and DPP-IV is inactivates the incretin hormone such glucagon-like peptide-1. As shown in Fig. 2A, B, CULE effectively inhibited DPP-IV and PTP-1B enzyme activities in a dose-dependent manner. At concentration of CULE 1000 μg/mL, the activity of both enzymes compared to control was significantly inhibited to 47.8 and 51.6%, respectively. Therefore, the action of CULE as PTP-1B and DPP-IV inhibitor can effectively enhance insulin secretion and glucose regulation.

Effect of CULE on cytotoxicity, NO production, and insulin secretion in RIN-m5F pancreatic beta cells

In the previous experiment, CULE did not show toxicity up to 400 μg/mL concentration in RIN-m5F pancreatic beta cells (Additional file 1: Fig. S1). After stimulation of RIN-m5F pancreatic beta cells with IL-1β and IFN-γ, cytotoxicity, NO production and insulin secretion were measured (Fig. 3). As a result, cell viability was significantly reduced to 53.3% in the treated control compared to the untreated normal cells. The cell viability was significantly increased to 63.04%, and 73.29% at the

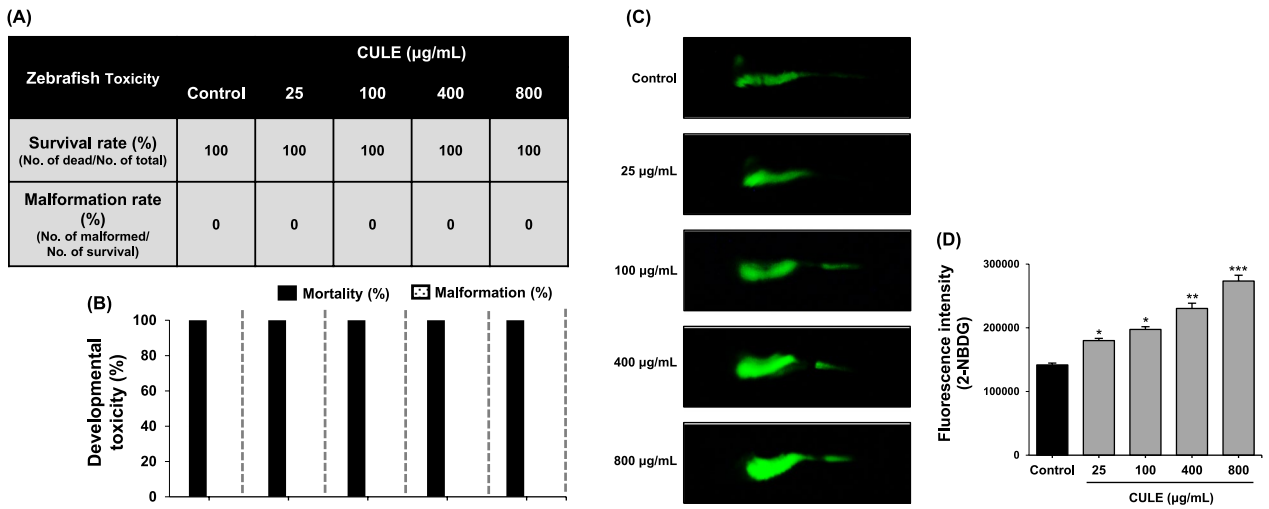

Fig. 1 Effect of CULE on mortality and malformation (**A**, **B**) and glucose uptake (**C**, **D**) in zebrafish larvae. Fertilized eggs were collected and placed in 96-well culture plates. Seven dpf, the larvae were treated with CULE for 24 h, and mortality and glucose uptake were observed. Each value is the mean ± SE of three independent repeated experiments. *p < 0.05, **p < 0.01, ***p < 0.001 vs. control

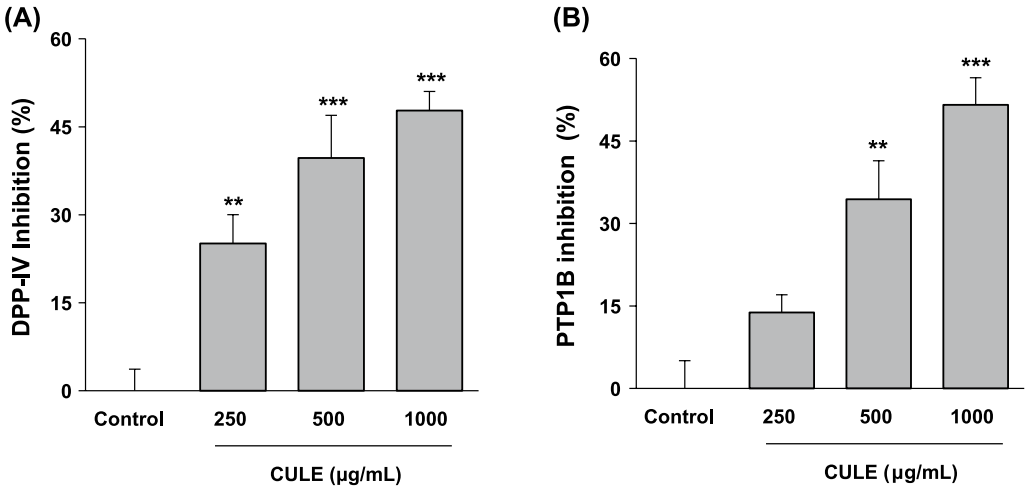

Fig. 2 Effect of CULE on DPP-IV (**A**) and PTP-1B (**B**) enzyme activities. Each value is the mean ± SE of four independent repeated experiments

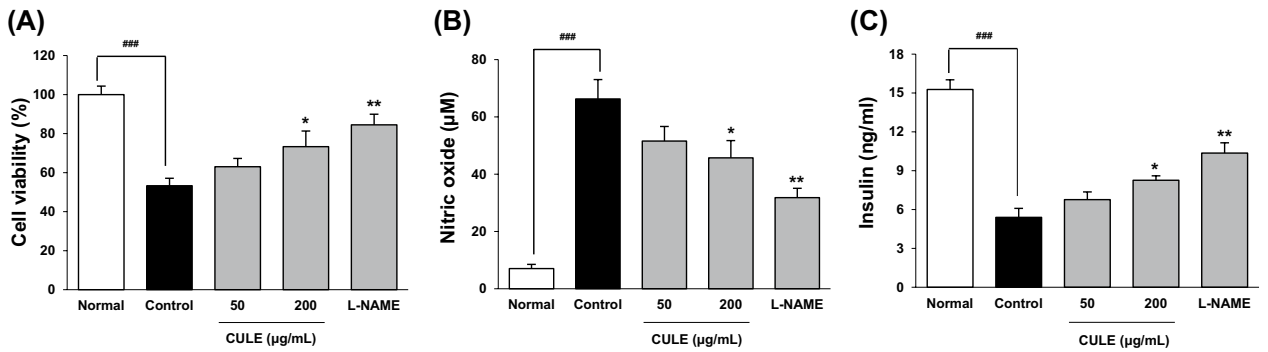

Fig. 3 Effect of CULE on cell viability (**A**), NO production (**B**), and insulin secretion (**C**) in cytokine-induced RINm5F pancreatic beta cells. RINm5F pancreatic beta cells were incubated with each concentration of CULE, IL-1β (2 ng/mL) and IFN-γ (100 U/mL) for 48 h. Cell viability was determined by the MTT assay. NO production was determined by a colorimetric assay. L-NAME (1 mM) was used as the positive control. Each value is the mean ± SE of four independent repeated experiments. $^{###}p < 0.001$ vs. untreated normal. $^{*}p < 0.05$, $^{**}p < 0.01$ vs. control

concentrations of CULE 50 and 200 μg/mL (Fig. 3A). The NO production was significantly increased to 66.29 μM in the control treated with IL-1β and IFN-γ compared to 7.06 μM in the normal without IL-1β and IFN-γ treatment (Fig. 3B). However, when CULE was treated at a concentration of 200 μg/mL, it was 45.71 μM, and L-NAME (1 mM) as a positive control was 31.83 μM. In the result of measuring insulin content, the control treated with IL-1β and IFN-γ was 5.40 ng/mL, which was significantly reduced compared to 15.27 ng/mL of the normal without IL-1β and IFN-γ (Fig. 3C). By treatment with CULE 200 μg/mL concentration, insulin secretion was 8.26 ng/mL and positive control L-NAME was 10.36 ng/mL, which was significantly increased compared to the control treated with IL-1β and IFN-γ.

Effect of CULE on cytotoxicity, glucose uptake, and mRNA expression in L6 myotubes

The addition of CULE up to 200 μg/mL concentration in L6 myotubes showed no cytotoxicity (Fig. 4A). The glucose uptake in cells treated with CULE at dose of 25, 50, 100, and 200 μg/mL was measured and only the CULE 25 μg/mL concentration showed a significant enhancement of glucose uptake compared to the untreated group (Fig. 4B). The glucose uptake of the positive control insulin was significantly increased to 1.46-fold. Treatment with CULE at 25 and 50 μg/mL significantly enhanced GLUT4 fluorescence intensity and mRNA expression compared to the control cells (Fig. 4C-E, G). Also, the expression of IRS-1 mRNA was significantly increased by treatment with

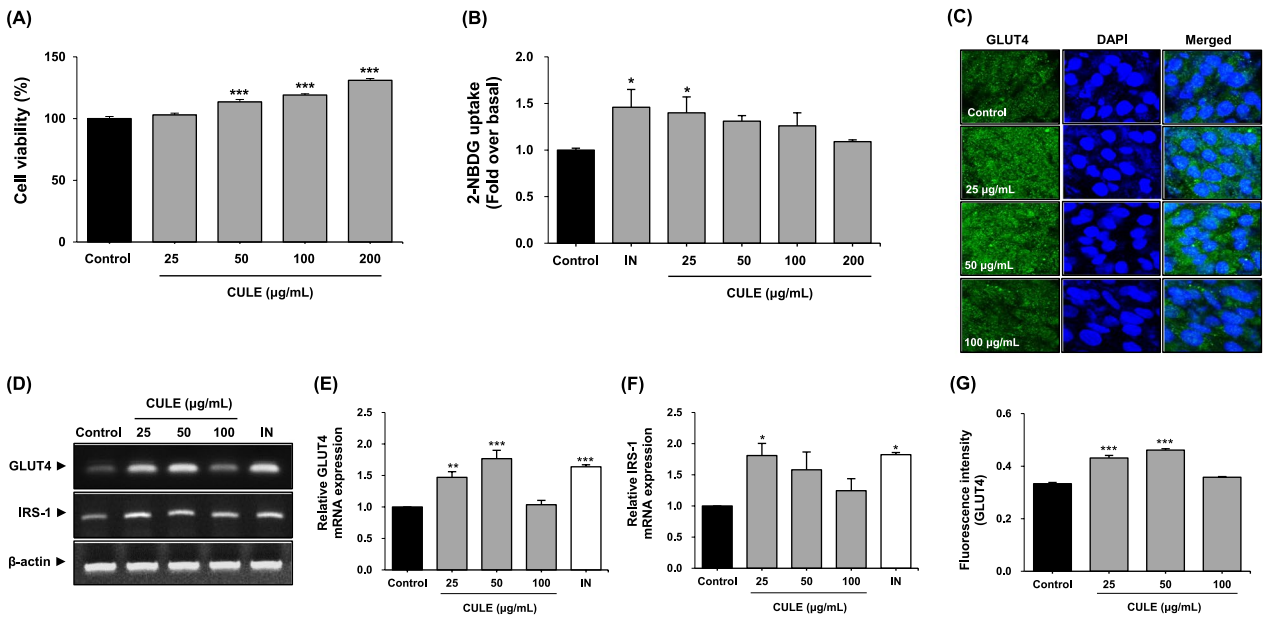

Fig. 4 Effect of CULE on cell viability (**A**), glucose uptake (**B**), immunofluorescence images and intensity of GLUT4 (**C**–**G**), and mRNA expression of GLUT4 and IRS-1 (**D**-**F**) in L6 myotubes. L6 myoblast were induced to differentiate with 2% horse serum. Cell viability was determined by the MTT assay. The quantitation of 2-NBDG uptake was assessed by the intracellular accumulation of fluorescence. Insulin (IN, 100 nM) was used as the positive control. Each value is the mean ± SE of three independent repeated experiments. *p < 0.05, **p < 0.01, ***p < 0.001 vs. control

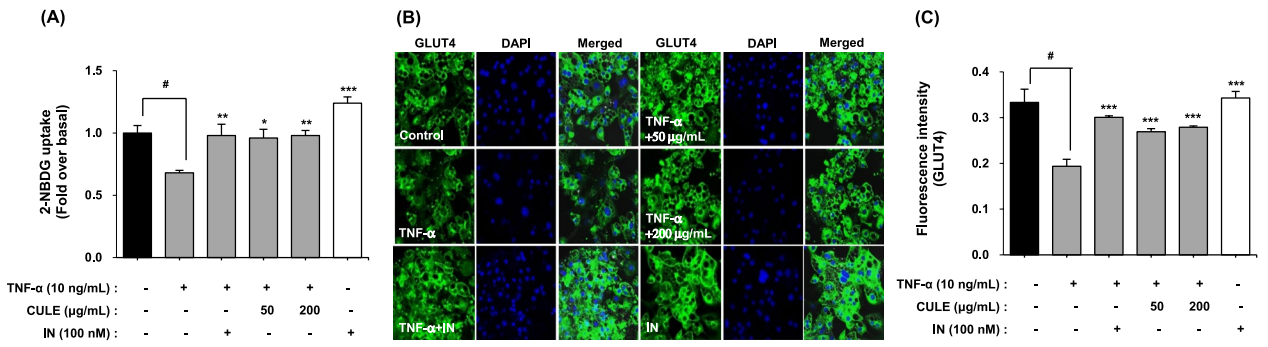

Fig. 5 Effect of CULE on glucose uptake (**A**), immunofluorescence images and intensity of GLUT4 (**B**, **C**) in the TNF-α-induced insulin-resistance model of 3T3-L1 adipocytes. Confluent 3T3-L1 preadipocytes were differentiated into adipocytes for eight days. Fully differentiated 3T3-L1 adipocytes were treated with TNF-α (10 ng/mL) for insulin resistance. After 48 h of TNF-α treatment, 2-NBDG uptake was assessed by the intracellular accumulation of fluorescence. IN (insulin, 100 nM) was used as the positive control. Each value is the mean ± SE of three independent experiments. #p < 0.001 vs. treatment without TNF-α. *p < 0.05, **p < 0.01, ***p < 0.001 vs. treatment with TNF-α

25 μg/mL CULE compared to the untreated group but slightly increased at concentration of 50 and 100 μg/mL (Fig. 4D, F).

Effect of CULE in TNF-α-induced insulin resistance model of 3T3-L1 adipocytes

CULE did not show toxicity up to 400 μg/mL concentration in 3T3-L1 adipocytes (Additional file 1: Fig. S1). In 3T3-L1 adipocytes, insulin resistance was induced by exposure to TNF-α (10 ng/mL), and was normally restored upon addition of insulin, enhancing the results of glucose uptake and GLUT4 fluorescence intensity (Fig. 5A, B). The treatment of CULE at 50 and 200 μg/mL significantly increase the glucose uptake and protein expression of GLUT4 in TNF-α-induced insulin resistance model of 3T3-L1 adipocytes (Fig. 5 B, C).

The expression levels of proteins that directly and indirectly affect insulin signaling and glucose metabolism

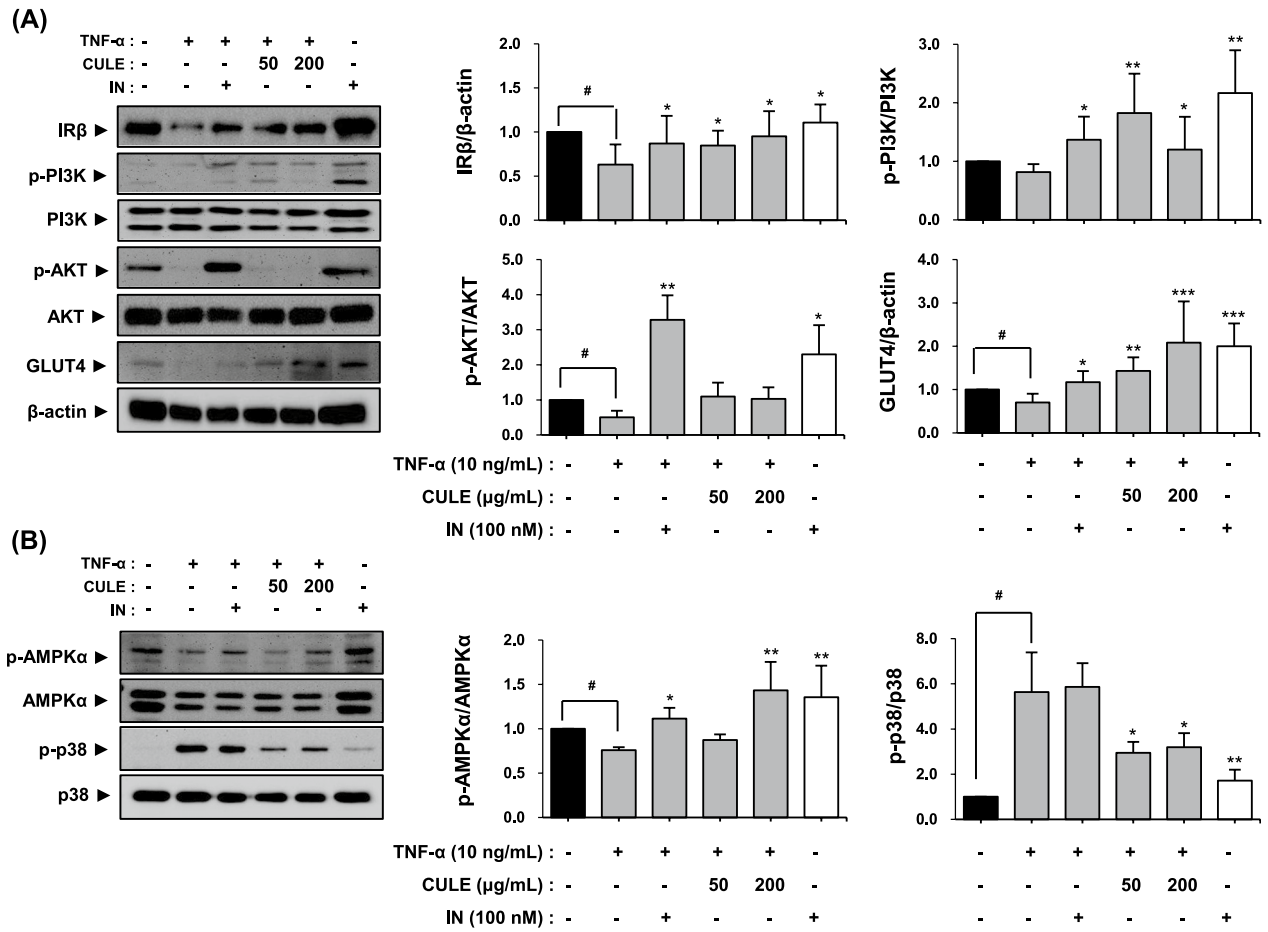

Fig. 6 Effect of CULE on the insulin-dependent signaling pathway (**A**) and AMPKα and p38 MAPK (**B**) in the TNF-α-induced insulin-resistance model of 3T3-L1 adipocytes. Confluent 3T3-L1 preadipocytes were differentiated into adipocytes for eight days. Fully differentiated 3T3-L1 adipocytes were treated with TNF-α (10 ng/mL) to induce insulin resistance. After 48 h of TNF-α treatment, protein expression was measured by Western blot analysis. IN (insulin, 100 nM) was used as the positive control. Each value is the mean ± SE of three independent repeated experiments. $^{\#}p < 0.001$ vs. treatment without TNF-α. $^{*}p < 0.05$, $^{**}p < 0.01$, $^{***}p < 0.001$ vs. treatment with TNF-α

were measured in TNF-α-induced insulin resistance model of 3T3-L1 adipocytes (Fig. 6). The expression of IRβ, p-PI3K, p-AKT, GLUT4, and AMPKα protein was significantly suppressed by the treatment of TNF-α compared to the untreated group (Fig. 6A). CULE (50 and 200 μg/mL) and insulin treatment significantly improved the expression of insulin signaling protein such as IRβ, p-PI3K, p-AKT, GLUT4, and AMPKα associated with glucose control and insulin response in TNF-α-induced insulin resistance model of 3T3-L1 adipocytes (Fig. 6), whereas the expression of p38 MAPK, which could be associated with insulin resistance, was effectively reduced by the treatment of CULE and insulin (Fig. 6B).

HPLC quantitation of quercetin in CULE

Quercetin compounds are widely distributed flavonoids in plants. Quercetin standard was purchased and analyzed by HPLC (Fig. 7). The quercetin component was separated under the above-described HPLC analysis conditions. Analysis of the HPLC spectrum of quercetin showed a peak retention time (tR) of 10.38 min and the UV spectrum showed maximum absorptions at 229.0, 254.2, and 367.2 nm. Several peaks were obtained from the HPLC analysis of CULE, but the presence of the quercetin component was confirmed by comparing the peak retention time with the standard sample. In the component profile of CULE, a peak with a retention time of 10.40 min, which was very similar to the quercetin of standard, and UV spectrum peaks with maximum absorptions at 224.3, 254.3, and 368.5 nm consistent with quercetin appeared. Based on the above results, quercetin was confirmed to be contained in CULE. The content of quercetin in CULE was determined to be 14.32 mg of quercetin per

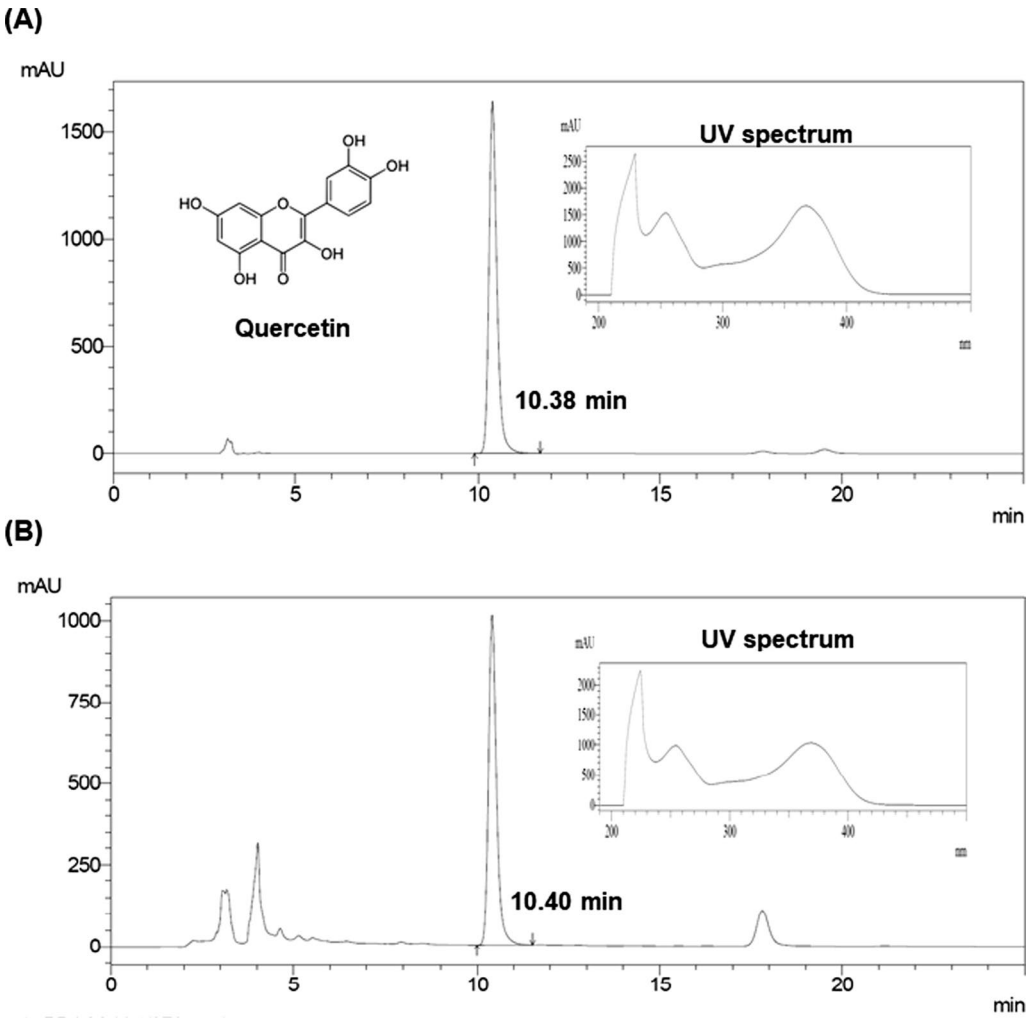

Fig. 7 HPLC chromatogram of quercetin (**A**) and CULE (**B**)

g of CULE using the calibration curve of the quercetin standard.

Discussion

C. unilocularis Buch-Ham leaf extract (CULE) has been traditionally used in Nepal and China, and is known to be effective for diabetes. However, there is little scientific evidences for antidiabetic effects of CULE. So, in this study, we scientifically verified the effect of CLUE on diabetes. We first reviewed the effect on glucose metabolism by CULE in zebrafish larvae. The zebrafish is an animal model that can be used to verify the efficacy of drug candidates for pathological studies and the treatment of metabolic diseases including diabetes [20, 21]. CULE showed increase in glucose uptake at all concentrations compared to the control in zebrafish larvae. Here, our results suggest that CULE are directly or indirectly involved in the regulation of glucose metabolism in an in vivo system.

In the cell free system, we measured the activation of biomarkers involved in insulin release and insulin sensitivity. We found a dose-dependent inhibitory effect on DPP-IV and PTP1B enzyme activities by CULE treatment. The cause of insulin resistance is not yet clear, but it is known to be caused by a variety of factors [22]. PTP1B interferes with the binding of IRS-1 to the insulin receptor beta region, which is an upstream signaling pathway in the insulin signaling pathway related to glucose metabolism, and thus interferes with the downstream of insulin signaling [23, 24]. Glucagon like peptide-1 (GLP-1) promotes insulin secretion in pancreatic beta cells and reduces glucagon secretion in pancreatic alpha cells to regulate glucose synthesis in the liver. However, GLP-1 is rapidly decomposed by DPP-IV in the human body, which causes problems in blood glucose regulation. Several DPP-IV inhibitors are available for the treatments of these glucose disorders [25]. In our study,

CULE effectively decreased the activity of PTP1B and DPP-IV enzymes, suggesting that it may become a potential therapeutic agent for T2D treatment.

In the cell system, we investigated the effect of CULE by inducing IL-1β and IFN-γ, which are known to induce dysfunction of pancreatic beta cells. As a result, in the CULE 200 μg/mL treatment group, the cell viability and the amount of insulin increased with a distinct decrease in NO production. Sharma et al. (2016, 2019) and Kim et al. (2016) reported that *Lespedeza cuneata* (G. Don), *Nelumbo nucifera* leaf, and *Tinospora cordifolia* stem extract increased insulin content and decreased NO production in RIN-m5F pancreatic beta cells treated with cytokines (IL-1β and IFN-γ) [14, 16, 26]. These results show that improvement of function of pancreatic beta cells induced the promotion of insulin secretion. Therefore, CULE is considered to have the potential to improve pancreatic beta cell dysfunction. Next, we examined the effect of CULE on glucose uptake in L6 myotubes. Muscle tissue plays a key role in regulating blood glucose levels and glycogen synthesis [27]. Wang et al. (2011) reported that antidiabetic effect of melon extract has been associated with the induction of IRS-1, PI3K, AKT and GLUT4 protein expression in the muscle tissue of mice [28]. CULE significantly increased glucose uptake and GLUT4 mRNA expression or fluorescence images in L6 myotubes. However, the results in cells did not show a concentration-dependent effect. Yin et al. (2008) reported that berberine action on glucose consumption in L6 and 3T3-L1 cells was independent of exposure time and concentration of insulin [29]. This suggests that the effect of CULE on GLUT4 protein expression and glucose uptake may differ depending on exposure concentration and time of CULE. Herein, our results suggest that glycemic regulation of CULE is related to translocation of the GLUT4 in L6 myotubes.

Finally, we constructed and reviewed an insulin resistance model by TNF-α treatment to investigate the effect of CULE on insulin resistance in 3T3-L1 adipocytes. It is well known that overexpression of TNF-α in adipose tissue contributes to the progression of insulin resistance [30]. In results, CULE significantly increased the expression of IRβ, PI3K, and GLUT4 on insulin signaling pathway in TNF-α-induced insulin resistance model of 3T3-L1 adipocytes. Moreover, the expression of p38 MAPK, which inhibits insulin signaling pathway, was markedly suppressed, and AMPKα expression, which is associated with insulin signaling activation, was significantly improved in this model. Taher et al. (2015) reported that α-mangostin component isolated from *Garcinia malaccensis* upregulates the expression of GLUT4 and leptin proteins, and induces an increase in glucose uptake in 3T3-L1 adipocytes [31]. Zhang et al. (2018) reported that *Astragali Radix* extract induces an increase of glucose uptake by increasing GLUT4 expression with AMPK activation [32]. Rosiglitazone (RSG) as a therapeutic agent for T2D in rat brown adipocytes is known to restore PI3K/AKT insulin signaling pathway and improve glucose uptake by impairing p38 and p42/p44 MAPK activation by TNF-α [33]. Thus, these results suggest that CULE ameliorate insulin resistance by TNF-α in 3T3-L1 adipocytes, restoring insulin signaling cascade IRβ/PI3K and insulin- or AMPKα-stimulated GLUT4 activation.

Conclusion

We found that CULE effectively promoted glucose uptake in zebrafish larvae. Also, CULE protected pancreatic beta cells from apoptosis induced by IL-1β and IFN-γ and improved insulin secretion. In skeletal muscle cells and adipocytes, CULE significantly regulated glucose metabolism and insulin resistance. Therefore, antidiabetic effect of CULE was closely associated with glucose metabolism via regulation of insulin secretion and sensitivity. Also, it has been shown that the antidiabetic effect of CULE is related to quercetin component, because the antidiabetic action of quercetin has already been elucidated [34–36]. However, it is necessary to conduct additional research on ingredients contained in CULE for the development of high-efficiency antidiabetic candidates. In conclusion, our findings suggest that CULE may be a useful material for the prevention and treatment of metabolic syndrome associated with T2D.

Abbreviations

AMPKα: 5′-AMP-activated protein kinase α; CULE: *Crateva unilocularis* leaf extract; Dpf: Days post-fertilization; DEPC: Diethylpyrocarbonate; DEX: Dexamethasone; DMEM: Dulbecco's modified eagle's medium; DPPH: 2,2-Diphenyl-1-picrylhydrazyl; DPP-IV: Dipeptidyl peptidase; ER: Estrogen receptor; FBS: Fetal bovine serum; GLP-1: Glucagon like peptide-1; GLUT4: Glucose transporter 4; HPLC: High-performance liquid chromatography; Hpf: Hours post-fertilization; HS: Horse serum; IBMX: 3-Isobutyl-1-methyxanthine; IRβ: Insulin receptor β; IRS-1: Insulin receptor substrate-1; IFN-γ: Interferon-γ; IDF: International diabetes federation; IL-1β: Interleukin-1β; IL-6: Interleukin-6; JNK: C-Jun N-terminal kinase; L-NAME: N omega-Nitro-L-arginine methyl ester hydrochloride; NBCS: Newborn calf serum; NO: Nitric oxide; MTT: 3-(4,5-Dimethylthiazol-2-yl) 2,5-diphenyltetrazolium bromide; PBS: Phosphate-buffered saline; PI3K: Phosphoinositide 3-kinases; PKC: Protein kinase C; PTP1B: Protein tyrosine phosphatase 1B; p38 MAPK: P38 mitogen-activated protein kinase; ROS: Reactive oxygen species; PCR: Polymerase chain reaction; RSG: Rosiglitazone; SDS: Sodium dodecyl sulfate; SNP: Sodium nitroprusside; TBARS: Thiobarbituric acid reactive substances; TGF-β: Transforming growth factor-β; Tris: Tris (hydroxymethyl) aminomethane; TNF-α: Tumor necrosis factor (TNF)-α; 2-NBDG: 2-(N-(7-nitrobenz-2-oxa-1,3-diazol-4-yl)-amino)-2-deoxyglucose.

Supplementary Information

The online version contains supplementary material available at https://doi.org/10.1186/s13765-022-00711-z.

Additional file 1: Figure S1. Effect of CULE on cell viability in 3T3-L1 adipocytes (A) and RIN-m5F pancreases beta cells (B).

Acknowledgements
This research was supported by research funds the Convergence Research Laboratory established by the Mokpo National University (MNU) Innovation Support Project in 2020 and the National Research Foundation of Korea (NRF) grant funded by the Korea government (MSIT) [No.2022R1A5A8033794].

Author contributions
Formal analysis, investigation, methodology, writing-original draft: C-MP; Formal analysis, writing-original draft: B-HJ; Formal analysis, methodology, writing-review, and editing: BRS; Formal analysis, writing-review, and editing: H-JK; Writing-review, and editing: D-WK; Conceptualization, supervision, writing-review, and editing: D-YR. All authors read and approved the final manuscript.

Declarations

Competing interests
The authors declare that they have no competing financial interests or personal relationships.

Author details
[1]Department of Nutraceutical Resources and Institute of Korean Herbal Medicine Industry, College of Natural Sciences, Mokpo National University, 1666, Youngsan-ro, Muan-gun, Jeonnam 58554, Republic of Korea. [2]College of Pharmacy, Mokpo National University, Jeonnam 58554, Republic of Korea. [3]Department of Biomedicine, Health & Life Convergence Sciences, BK21 FOUR, Mokpo National University, Jeonnam 58554, Republic of Korea. [4]Inhalation Toxicity Research Group, Korea Institute of Toxicology, Jeongeup-si, Jeollabuk-do 56212, Republic of Korea.

Received: 23 December 2021 Accepted: 9 June 2022
Published online: 12 July 2022

References

1. Arneth B, Arneth R, Shams M (2019) Metabolomics of type 1 and type 2 diabetes. Int J Mol Sci 20:2467
2. Ozougwu JC, Obimba KC, Belonwu CD, Unakalamba CB (2013) The pathogenesis and pathophysiology of type 1 and type 2 diabetes mellitus. J Physiol Pathophysiol 4:46–57
3. Petersen MC, Shulman GI (2018) Mechanisms of insulin action and insulin resistance. Physiol Rev 98:2133–2223
4. Sharma BR, Kanneganti TD (2021) NLRP3 inflammasome in cancer and metabolic diseases. Nat Immunol 22:1–10
5. Zhang BB, Moller DE (2000) New approaches in the treatment of type 2 diabetes. Curr Opin Chem Biol 4:461–467
6. Van Belle TL, Coppieters KT, Von Herrath MG (2011) Type 1 diabetes: etiology, immunology, and therapeutic strategies. Physiol Rev 91:79–118
7. Elbelt U (2018) Diabetes mellitus type 2: recent publications and new drugs. Deutsch Med Wochenschr 143:772–776
8. Hu C, Jia W (2019) Therapeutic medications against diabetes: what we have and what we expect. Adv Drug Deliv Rev 139:3–15
9. Zheng XH, Duan HC, Li SM, Dong Q (2021) The complete chloroplast genome of *Crateva unilocularis* (Capparaceae). Mitochondrial DNA B Resour 6:658–659
10. Ma Q, Chen Y, Zhang X, Cai S, Sun Y, Ma N, Yi J (2022) Crateva unilocularis Buch. shoots attenuate d-galactose-induced brain injury and cognitive disorders of mice through the PI3K/Akt/Nrf2 pathway. Food Funct 13:3465–3480
11. Gazioglu I, Semen S, Acar OO, Kolak U, Sen A, Topcu G (2020) Triterpenoids and steroids isolated from anatolian capparis ovata and their activity on the expression of inflammatory cytokines. Pharm Biol 58:925–931
12. Malla B, Gauchan DP, Chhetri RB (2014) Medico-ethnobotanical investigations in parbat district of Western Nepal. J Med Plants Res 8:95–108
13. Zingue S, Yaya AJG, Michel T, Ndinteh DT, Rutz J, Auberon F, Maxeiner S, Chun FKH, Tchinda AT, Njamen D, Blaheta RA (2020) Bioguided identification of daucosterol, a compound that contributes to the cytotoxicity effects of *Crateva adansonii* DC (capparaceae) to prostate cancer cells. J Ethnopharmacol 247:112251
14. Sharma BR, Park CM, Kim HA, Kim HJ, Rhyu DY (2019) *Tinospora cordifolia* preserves pancreatic beta cells and enhances glucose uptake in adipocytes to regulate glucose metabolism in diabetic rats. Phytother Res 33:2765–2774
15. Park CM, Kim KT, Rhyu DY (2021) Exposure to a low concentration of mixed organochlorine pesticides impairs glucose metabolism and mitochondrial function in L6 myotubes and zebrafish. J Hazard Mater 414:125437
16. Sharma BR, Kim MS, Rhyu DY (2016) *Nelumbo Nucifera* leaf extract attenuated pancreatic β-cells toxicity induced by interleukin-1β and interferon-γ, and increased insulin secrection of pancreatic β-cells in streptozotocin-induced diabetic rats. J Tradit Chin Med 36:71–77
17. Manandhar B, Kim HJ, Rhyu DY (2020) *Caulerpa okamurae* extract attenuates inflammatory interaction, regulates glucose metabolism and increases insulin sensitivity in 3T3-L1 adipocytes and RAW 264.7 macrophages. J Integr Med 18:253–264
18. Sharma BR, Kim HJ, Rhyu DY (2015) *Caulerpa lentillifera* extract ameliorates insulin resistance and regulates glucose metabolism in C57BL/KsJ-db/db mice via PI3K/AKT signaling pathway in myocytes. J Transl Med 13:62
19. Sharma BR, Rhyu DY (2014) Anti-diabetic effects of *Caulerpa lentillifera*: stimulation of insulin secretion in pancreatic β-cells and enhancement of glucose uptake in adipocytes. Asian Pac J Trop Biomed 4:575–580
20. Zang L, Shimada Y, Nishimura N (2017) Development of a novel zebrafish model for type 2 diabetes mellitus. Sci Rep 7:1461
21. Zang L, Maddison LA, Chen W (2018) Zebrafish as a model for obesity and diabetes. Front Cell Dev Biol 6:91
22. Shibata M, Hakuno F, Yamanaka D, Okajima H, Fukushima T, Hasegawa T, Ogata T, Toyoshima Y, Chida K, Kimura K, Sakoda H, Takenaka A, Asano T, Takahashi SI (2010) Paraquat-induced oxidative stress represses phosphatidylinositol 3-kinase activities leading to impaired glucose uptake in 3T3-L1 adipocytes. J Biol Chem 285:20915–20925
23. Zhang ZY, Lee SY (2003) PTP1B inhibitors as potential therapeutics in the treatment of type 2 diabetes and obesity. Expert Opin Investig Drugs 12:223–233
24. Tian C, Chang H, La X, Li JA (2017) *Wushenziye* formula improves skeletal muscle insulin resistance in type 2 diabetes mellitus via PTP1B-IRS1-Akt-GLUT4 signaling pathway. Evid Based Complement Alternat Med 2017:4393529
25. Green BD, Flatt PR, Bailey CJ (2006) Dipeptidyl peptidase IV (DPP IV) inhibitors: a newly emerging drug class for the treatment of type 2 diabetes. Diab Vasc Dis Res 3:159–165
26. Kim MS, Sharma BR, Rhyu DY (2016) Beneficial effect of *Lespedeza cuneata* (G. don) water extract on streptozotocin-induced type 1 diabetes and cytokine-induced beta-cell damage. Nat Prod Sci 22:175–179
27. Bonadonna RC, Saccomani MP, Del Prato S, Bonora E, DeFronzo RA, Cobelli C (1998) Role of tissue-specific blood flow and tissue recruitment in insulin-mediated glucose uptake of human skeletal muscle. Circulation 98:234–241
28. Wang ZQ, Zhang XH, Yu Y, Poulev A, Ribnicky D, Floyd ZE, Cefalu WT (2011) Bioactives from bitter melon enhance insulin signaling and modulate acyl carnitine content in skeletal muscle in high-fat diet-fed mice. J Nutr Biochem 22:1064–1073
29. Yin J, Gao Z, Liu D, Liu Z, Ye J (2008) Berberine improves glucose metabolism through induction of glycolysis. Am J Physiol Endocrinol Metab 294:E148-156
30. Cawthorn WP, Sethi JK (2008) TNF-alpha and adipocyte biology. FEBS Lett 582:117–131
31. Taher M, Mohamed Amiroudine MZ, Tengku Zakaria TM, Susanti D, Ichwan SJ, Kaderi MA, Ahmed QU, Zakaria ZA (2015) α-Mangostin improves glucose uptake and inhibits adipocytes differentiation in 3T3-L1 cells via PPARγ, GLUT4, and leptin expressions. Evid Based Complement Alternat Med 2015:740238

32. Zhang R, Qin X, Zhang T, Li Q, Zhang J, Zhao J (2018) *Astragalus* polysaccharide improves insulin sensitivity via AMPK activation in 3T3-L1 adipocytes. Molecules 23:2711
33. Hernandez R, Teruel T, de Alvaro C, Lorenzo M (2004) Rosiglitazone ameliorates insulin resistance in brown adipocytes of Wistar rats by impairing TNF-alpha induction of p38 and p42/p44 mitogen-activated protein kinases. Diabetologia 47:1615–1624
34. Chen S, Jiang H, Wu X, Fang J (2016) Therapeutic effects of quercetin on inflammation, obesity, and type 2 diabetes. Mediators Inflamm 2016:9340637
35. Eid M, H, S Haddad P, (2017) The antidiabetic potential of quercetin: underlying mechanisms. Curr Med Chem 24:355–364
36. Sato S, Mukai Y (2020) Modulation of chronic inflammation by quercetin: the beneficial effects on obesity. J Inflamm Res 13:421–431

Publisher's Note